



EFFECT OF A THERMOPLASTIC ELASTOMER COMPATIBILIZER (SEBS-g-MAH) ON THE PROPERTIES OF PP/PET BLENDS

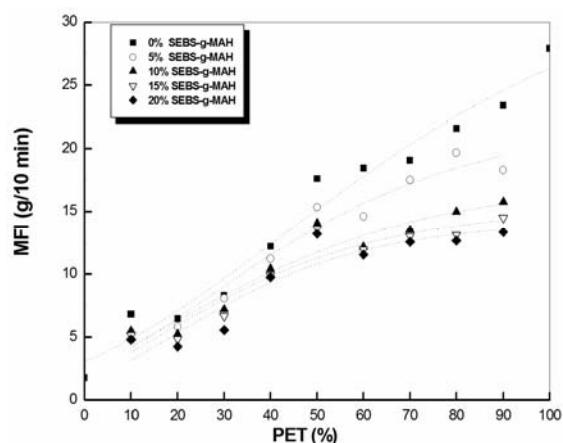
Ismahane DEBBAH,^{a*} Rachida KRACHE,^a Khalida BELKOUISSEM,^a Djafer BENACHOUR^a and Maria Esperanza CAGIAO^b

^aLaboratoire des Materiaux Polymericque Multiphasique, Département de Génie des Procédés, Faculté de Technologie, Université Ferhat Abbas, Sétif 19000, Algérie

^bInstituto de Estructura de la Materia, Consejo Superior de Investigaciones Científicas Serrano 119, 28006 Madrid, Spain

Received February 23, 2017

Polyethylene terephthalate (PET) and polypropylene (PP) are widely used and frequently encountered in domestic and industrial plastics, especially in the soft drink bottles. In the present work, different compositions of PP/PET blends were prepared and compatibilized by various contents of SEBS-g-MAH. The compatibilizing efficiency was examined using macro- (tensile and impact strength) and micro-mechanical testing (microhardness measurement), differential scanning calorimetry (DSC), wide-angle X-ray scattering (WAXS), and melt flow index (MFI) determinations. The results show that the addition of SEBS-g-MAH improves the processability and the toughness of these blends. The changes in the melting enthalpies (ΔH_m) of the PP and PET components and the decrease of MFI values in the compatibilized blends indicated enhanced interactions between the discrete PET and PP phases induced by the functional compatibilizer. The DSC crystallinity of each component depended on the blend composition, and was slightly influenced by the presence of the compatibilizer. In the samples subjected to compression molding, the WAXS crystallinity of PP component slightly decreased in the presence of increasing amounts of compatibilizer.



INTRODUCTION

Polymer blends offer an interesting way to modify the properties of thermoplastics and to lower the cost of engineering high performance polymers. The problem encountered is that most of blends are immiscible and have poor mechanical properties compared to their components due to unfavorable interactions which exist at the molecular level. This leads to a great interfacial tension, which makes dispersion of the components during mixing difficult.

Unfavorable interactions lead to an unstable morphology (coalescence of phases) and to a poor interfacial adhesion.

Poly(ethylene terephthalate) is an important engineering thermoplastic polyester because of its good combination of properties, such as good thermal and mechanical properties, as well as excellent chemical resistance, and good optical and barrier properties.¹ However, the notched impact strength of PET is very low, and this is not desired in engineering thermoplastics. The improvement of

* Corresponding author: debbah.isma@gmail.com

the notched impact behavior can be achieved by incorporating an elastomeric material, the basis of the improvement being the better dispersion of the small rubber particles.²

On the other hand, the properties of polyolefins may be improved by blending them with thermoplastic polyesters or polyamides.^{1,3,4} Polyesters are of particular interest, because they exhibit lower moisture absorption. PET and PP are incompatible due to their differences in chemical nature and polarity. Their blends exhibit a clear two-phase morphology, where the dispersed phase forms large spherical droplets, and no adhesion between the two phases exists. Generally, the strength and stiffness of their blends increases with increasing PET content but, due to the incompatibility, the blends exhibit poor impact strength.⁵ These PP/PET blends were studied in the last decade with the objective of obtaining new materials with modulated properties, depending on composition and phase morphology. But, in order to obtain stable materials with good properties, the blends have to be compatibilized.⁶⁻⁸

In this work, we have investigated the effects of the compatibilization on the structure, and on the rheological, thermal and mechanical properties of blends of PET and PP. The compatibilizer used in this study is a triblock copolymer consisting of polystyrene end-blocks and poly(ethylene-butylene) mid-blocks grafted with maleic anhydride, SEBS-g-MAH. This copolymer was already used to compatibilize other blends of polar and apolar polymers with satisfactory results.⁹⁻¹² The efficiency of the compatibilization is determined as a function of the compatibilizer content.

EXPERIMENTAL

Materials

The following materials were used in this investigation:

Polypropylene PP random copolymer, containing 8 wt. % of polyethylene: Moplen RP241H, supplied by Basell. Density: 0.9 g/cm³; melt index: 1.8 g/10 min (at 230 °C and under a load of 2.16 kg).

Polyethylene terephthalate PET (medium viscosity extrusion grade): Eslon PET-3212 produced by Saehan Industries. Intrinsic viscosity: 0.82 dl/g; density: 1.4 g/cm³.

SEBS-g-MAH compatibilizer: Kraton FG-1901X, supplied by Shell Chemicals, The Hague, Netherlands. This is a styrene-ethylene/butylene-styrene block copolymer functionalized with 2 wt. % of maleic anhydride. Characteristics: Average $M_w \approx 200,000$; styrene/rubber ratio: 28/72; density: 0.919 g/cm³; melt index: 3.2 g/10min; T_g: -42°C.

The compositions of the studied PP/PET blends were: 100/0, 90/10, 80/20, 70/30, 60/40, 50/50, 40/60, 30/70, 20/80, 10/90, 0/100 wt. %. The amounts of the compatibilizer added (5, 10, 15 and 20 wt. %) were calculated with respect to the total blend weight.

Blending and Compression Molding

Before blending, PET was dried in a dehumidifying dryer for 24 hours at 100 °C. Melt blending of the dry mixed materials was done in a Controlab rotating single screw extruder having a diameter of 25 mm. The temperature profile used was: 240-250-265 °C; the screw speed was 50 turns/min. The extruded blends were cooled at room temperature in air. Thereafter, the pelletized and dried blends were molded to tensile and impact bar tests by compression in a hydraulic press at 265 °C and 220 kg/cm² for 5 min.

It is important to stress out that the calorimetric study has been performed on the extruded samples. However, to carry out the WAXS study and the hardness measurements the samples had to be previously subjected to a compression molding process under the following conditions: T = 275 °C; pressure: 5 bar; time: 4 min. This cycle was repeated twice on each sample. Of course, the molding process completely erased the previous thermal story of the samples. This is a very important aspect to take into account when one compares the results of the different studies. Thus, in all the samples analyzed by DSC, the PET component is crystalline, showing the corresponding melting maximum. On the contrary, in all the compression molded samples, the PET appears to be amorphous, at least from the X-ray diffraction point of view. In relation to this, it is noteworthy to indicate that some of the compression molded samples without compatibilizer showed an evident separation of phases, even by visual inspection. In the microhardness study we tried to measure the hardness of the two phases, wherever it was possible.

Techniques

Wide Angle X-ray Diffraction (WAXS) study

The wide-angle X-ray scattering (WAXS) study was carried out with a Seifert (Ahrensburg, Germany) diffractometer working in the reflection mode. The experimental conditions were the following: Ni-filtered CuK_α radiation with a wavelength $\lambda = 0.15418$ nm, 40 kV and 35 mA, angular range (2θ) = 5–35°, and scan rate = 0.02°/s. The WAXS-determined crystallinity (α_{WAXS}) of every sample was calculated as the ratio of the area corresponding to the crystalline peaks to the total area of the diffractogram.

Differential scanning calorimetry (DSC) study

The thermal study was performed using a Perkin Elmer (Norwalk, Connecticut, USA) DSC-7 differential scanning calorimeter (DSC) instrument in an inert N₂ atmosphere. Sample weights were 2–12 mg. The temperature range studied was 40–300 °C. The heating rate was 10°C/min. The crystallinity α_{DSC} was derived from the melting enthalpy obtained by DSC according to the following expression:

$$\alpha_{DSC} = \Delta H_m / \Delta H_m^\infty \quad (1)$$

where ΔH_m and ΔH_m^∞ are the experimental melting enthalpy and the melting enthalpy for an infinitely thick crystal, respectively.

Rheological properties

Melt flow index of both the neat polymers and the blends was measured with a Melt-Indexer model 5 under a load of 2.16 kg, at 260 °C and using a die with length to diameter ratio (L/D) of 5/2. The measurements were done according to ASTM D1238 standard, and the MFI values were derived through the following expression:

$$MFI = 600m/t \quad (\text{g}/10\text{min}) \quad (2)$$

where m is the extruded mass (in g) and t is the measurement time (in min).

Macro- and micromechanical properties

Before performing the mechanical properties, the test bars were conditioned for 24 h at 100 °C. Tensile test (ASTM-632 standard) was carried out at room temperature using a ZWICK model Prufung 1445 testing machine, assisted with a computer. The force sensor was 2000 Newton and a crosshead speed of 50 mm/min was used.

Izod impact test was performed on notched and unnotched specimens (ISO R-180 standard) using a CEAST pendulum, equipped with a 7.5 Joule hammer.

Microhardness H was determined at room temperature in the compressed samples with a Leitz (Wetzlar, Germany) microindentation tester with a square-based diamond indenter. The H value was derived from the residual projected area of indentation according to the following expression:¹³

$$H = kP/d^2 \quad (3)$$

where d is the length of the impression diagonal in m, P is the contact load applied in N, and k is a geometrical factor equal to 1.854. Loads of 0.5 and 1 N were applied. The loading cycle was 0.1 min. From 8 to 10 indentations were performed on the surface of each sample, and the results were averaged.

RESULTS AND DISCUSSION

Wide Angle X-ray Diffraction (WAXS) results

In all the samples analyzed by DSC the PET component is crystalline, showing the corresponding melting maximum. On the contrary, in all the compression molded samples, the PET appears to be amorphous, at least from the X-ray diffraction point of view (diffractograms not shown here).

Some of the uncompatibilized molded samples showed an evident separation of phases, even by visual inspection. For the WAXS study, we selected the samples pieces in such a way that the two phases were more or less averaged.

As the PET component is unable to crystallize under these conditions, the WAXS crystallinity of all series of samples varies linearly with the PET content (see Figure 1). It seems that the presence of the compatibilizer slightly decreases the iPP crystallinity. This effect is more pronounced for higher compatibilizer content.

Differential scanning calorimetry (DSC) study

The results obtained in the calorimetric study show that the melting temperatures of both polymers PP and PET are practically constant for all compositions, both in pure and compatibilized blends (thermograms not shown here). Thus, for the PP component, is $T_m = 137-141$ °C, and for the

PET component, is $T_m = 246-251$ °C. This indicates that the crystal thickness of the components, l_c , derived from the Thomson-Gibbs equation (eq. 4), was neither affected by the blending process nor by the addition of the compatibilizer:

$$T_m = T_m^0 [1 - (2\sigma_e / \Delta H_m^\infty l_c)] \quad (4)$$

In this equation, σ_e is the surface free energy and T_m^0 is the equilibrium melting point of each component. On the other hand, ΔH_m^∞ is the value of the melting enthalpy for an infinitely thick crystal corresponding to each component. For the PP, we have taken the following values: $T_m^0 = 187.7$ °C,¹⁴ $\Delta H_m^\infty = 207.33$ J/g¹⁴ and $\sigma_e = 100$ erg/cm².¹⁵ For the PET, we used $T_m^0 = 280$ °C¹⁴, $\Delta H_m^\infty = 140.1$ J/g¹⁴ and $\sigma_e = 151-161$ erg/cm².¹⁶ The l_c values obtained from eq. (4) for both components were 24-29 nm for the PET and 9-10 nm for the PP.

In all the studied blends, the crystallinity α_{DSC} of each component depends only on the composition. Thus, as the PP content increases, its crystallinity also increases whereas PET crystallinity decreases. The behavior of pure blends and blends with 5 % SEBS-g-MAH is shown in Figs. 2a and 2b, respectively. Total crystallinity, obtained by adding the contributions of both components vary between 32 and 37 % (pure blends, Fig. 2a) or between 30 and 34 % (blends with 5 % SEBS-g-MAH, Fig. 2b). Blends with 10 and 15 % of compatibilizer (results not shown here) behave in a similar way.

The large difference observed between α_{DSC} and α_{WAXS} can be explained taking into account that the calorimetric study has been performed directly upon the extruded samples. However, as it was indicated above, the WAXS and hardness studies have been done after subjecting the extruded samples to a compression molded process, which completely erased their previous thermal story.

The decrease observed in the melting enthalpies of the polymer components in the compatibilized blends as compared to the pure ones (see Table 1) is probably due to the influence of the compatibilizer, constituted by amorphous chains, that reduce the crystallization ability of, both, PP and PET. This effect increases for higher compatibilizer content. It can be assumed that an increase of the amorphous portion of polymer in the blend is proportional to the internal surface on the boundary of PP/PET. These results can also be explained by considering both the effect of the compatibility of the SEBS tri-block with the PP phase and that of chemical reactions of anhydride functional group with PET at the interface in the melt.^{5,17}

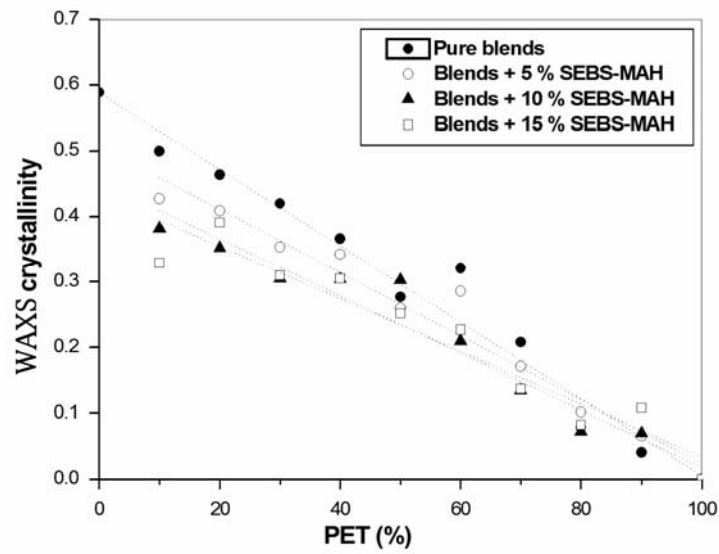


Fig. 1 – WAXS crystallinity α_{WAXS} of pure and compatibilized PP/PET blends as a function of the PET content.

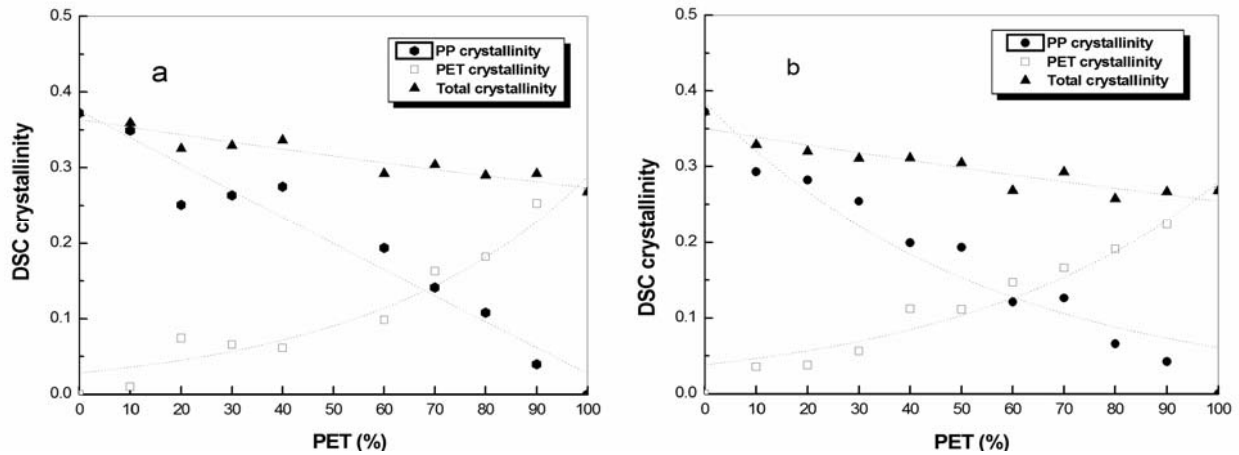


Fig. 2 – α_{DSC}^{PP} , α_{DSC}^{PET} and total α_{DSC} in: a) PP/PET pure blends; b) blends containing 5 % of SEBS-g-MAH as a function of the PET conten.

Table 1

PP and PET melting enthalpies for pure and compatibilized PP/PET blends

The table	Pure PP/PET blends		PP/PET blends + 5 % SEBS-G-MAH		PP/PET blends + 10 % SEBS-G-MAH		PP/PET blends + 15% SEBS-G-MAH	
	ΔH_m PP (J/g)	ΔH_m PET (J/g)	ΔH_m PP (J/g)	ΔH_m PET (J/g)	ΔH_m PP (J/g)	ΔH_m PET (J/g)	ΔH_m PP (J/g)	ΔH_m PET (J/g)
%PET								
0	77.2	-	77.2	-	77.2	-	77.2	-
10	72.4	1.4	60.8	5.0	59.7	3.3	42.2	8.8
20	52.1	10.4	58.5	5.3	53.3	6.1	49.9	3.7
30	54.7	9.2	52.7	7.9	36.8	15.7	43.9	5.5
40	57.1	8.6	41.3	15.7	39.1	12.4	29.6	16.0
50	38.2	15.1	40.1	15.6	9.8	22.6	33.6	13.7
60	40.2	13.8	25.1	20.6	11.1	16.8	27.4	16.0
70	29.3	22.8	26.2	23.3	7.8	17.3	14.4	24.4
80	22.4	25.5	13.7	26.8	17.7	22.7	9.4	27.1
90	8.2	35.4	8.8	31.4	12.0	26.5	17.2	25.2
100	-	37.6	-	37.6	-	37.6	-	37.6

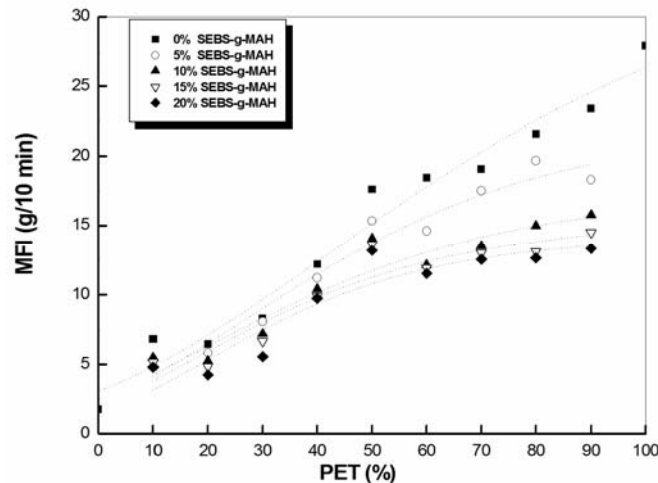


Fig. 3 – Melt flow index MFI of PP/PET blends with and without SEBS-g-MAH compatibilizer as a function of the PET content.

Rheological Properties

Figure 3 shows the dependence between the melt flow index of the PP/PET blends and both the PET and the SEBS-g-MAH contents. The MFI of PP/PET blends appears to vary gradually and monotonically from the value of the PP to that of the PET. The addition of the compatibilizer leads to a decrease of MFI with increasing SEBS-g-MAH content; this decrease is more pronounced for PET content from 50 to 90 wt. %. The decrease of the MFI, especially at high content of the functionalized rubber, cannot be attributed to the presence of the SEBS-g-MAH, because of its low viscosity compared with the two other components. This decrease must be attributed to the enhanced interactions between the discrete PP and PET phases induced by the functionalized rubber.^{5,17}

Mechanical Properties

Figure 4 shows the relationship between the PET content and the Young's modulus E for the different pure and compatibilized PP/PET blends. Pure PP has an E value of 4.5 GPa, and pure PET a value of 7.16 GPa. The modulus of the pure PP/PET blends decreases with the increase in the PET content until 60 wt. % PET; then, an abrupt increase is observed, until E reaches the value of pure PET. This can be due largely to the debonding of the PET particles, after that the particles will contribute little to the overall modulus.

The effect of the compatibilizer content on the Young's modulus is also illustrated in figure 4, as it was mentioned previously. For a PET content equal or higher than 50 wt. %, an improvement on

the E value is obtained. This improvement is higher when decreasing the SEBS-g-MAH content.

Figure 5 shows the variation of stress-at-break σ_r as a function of the wt% of PET and the SEBS-g-MAH content. The strength of PET is slightly higher than that of PP, adding up to 50% of PET does not improve significantly the strength of the blends. This can be attributed to the poor interfacial bonding between the polymers. From Figs. 4 and 5, it can be observed that the E and the σ_r dependence on composition for pure blends show a negative deviation, i.e., the blend properties lie below the additivity line. This negative deviation is due to the poor interfacial adhesion between the homopolymer phases, which causes poor stress transfer between the matrix and the dispersed phase. An abrupt change in the slope of the E and the σ_r curves is seen between the PP/PET compositions from 40/60 to 30/70. This change in slope can be explained in terms of a change in morphology of the blends.^{5,17} From 60 wt. % PET onwards, the PP is dispersed as domains in the continuous PET phase. Therefore, the observed change in slope for pure blends can be attributed to a phase inversion of PET from the dispersed phase to the continuous phase.

In Fig. 5, the observed increase in the tensile strength σ_r of compatibilized blends as a function of PET content is due to the improvement of compatibility between PET and PP and to the hard plastic phase of PET matrix. However this improvement is higher when decreasing the SEBS-g-MAH content. Figures 4 and 5 clearly highlight that the presence of the functionalized rubber induces brittle-ductile transition, thus yielding a ductile material. The decrease of the tensile

strength and Young's modulus as the compatibilizer content increases is expected because the SEBS-g-MAH is rubbery in nature¹⁷ and shows low values of these ultimate properties.

The variation of strain at break, or elongation at break ϵ_r (in %) with the blend composition is shown in Figure 6. The strain at break of pure PP/PET blends is found to decrease quickly with the addition of 10 wt. % PET then it becomes constant and equal to that of pure PET. The poor interfacial adhesion between the homopolymers is

reflected in the poor elongational property of the blends; the lack of adhesion between the components results in the formation of PP agglomerates in the PET matrix, thus leading to a premature failure, and to a low elongation at break. A significant improvement is obtained with 20 wt. % SEBS-g-MAH for the compatibilized blends, especially at high PP weight contents. This behavior could be the result of the rubbery nature of SEBS-g-MAH and the extent of the interfacial adhesion as a result of compatibilization.

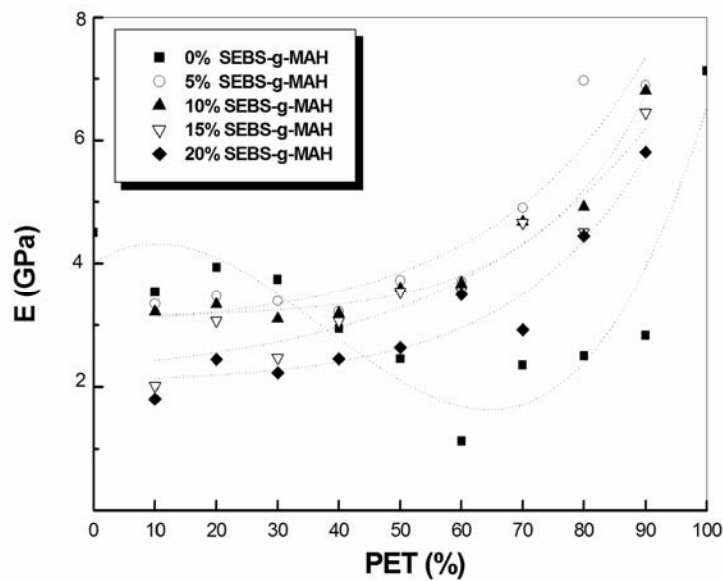


Fig. 4 – Young's modulus E of PP/PET blends, pure and compatibilized with SEBS-g-MAH, as a function of the PET content.

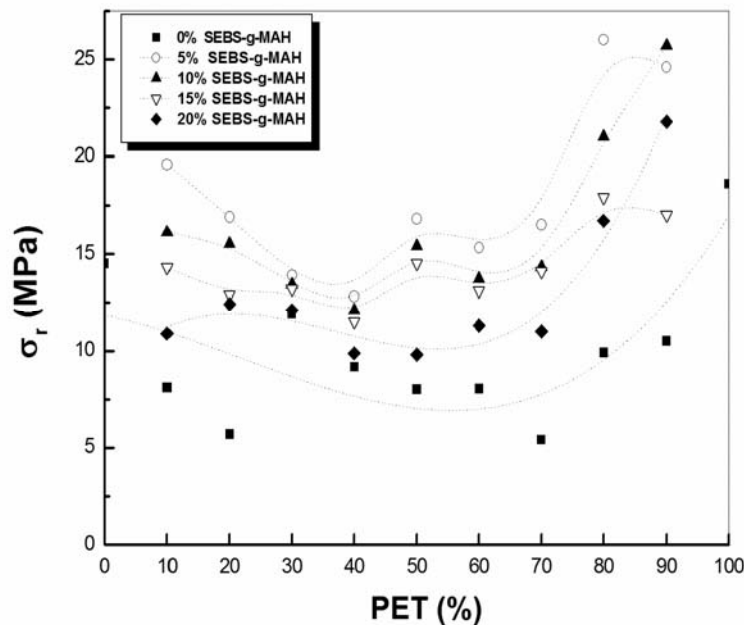


Fig. 5 – Tensile stress at break σ_r of PP/PET blends, pure and compatibilized with SEBS-g-MAH, as a function of the PET content.

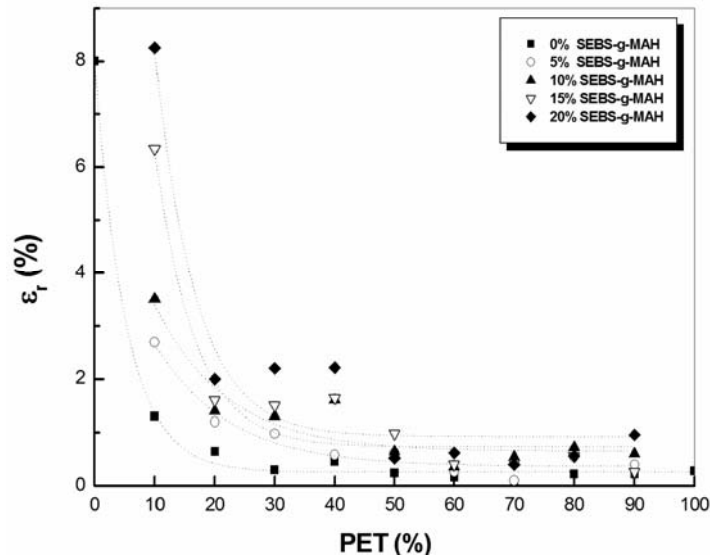


Fig. 6 – Tensile strain at break ϵ_t of PP/PET blends, pure and with SEBS-g-MAH compatibilizer, as a function of the PET content.

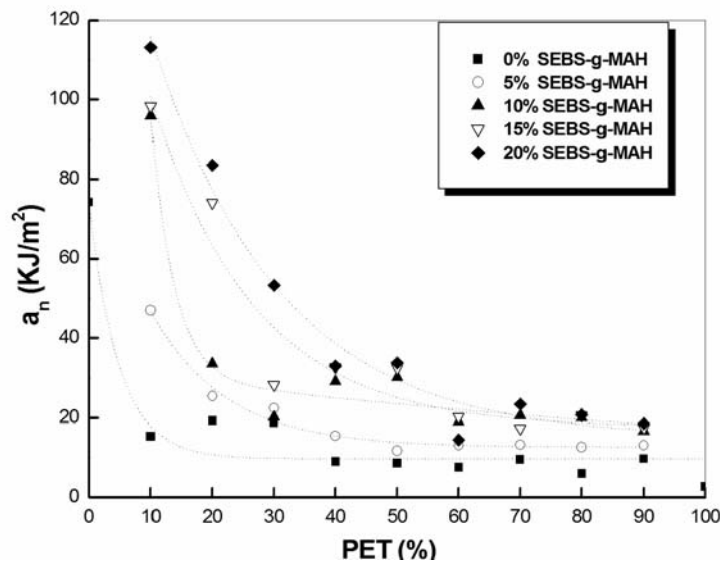


Fig. 7 – Notched Izod impact strength a_n of PP/PET blends, pure and with SEBS-g-MAH, as a function of the PET content.

The impact properties of PP/PET blends are presented in Figure 7. The notched Izod impact strength (a_n) of PP decreases dramatically with the addition of 10 wt.% PET. Immiscibility causes weak interfacial adhesion between the PET phase and the PP phase; the larger PP particles dispersed in the PET matrix give rise to a decreased impact strength in the blends. However, this property is highly improved by the presence of SEBS-g-MAH in the blends, thus increasing with increasing compatibilizer content. In fig. 7 it can be observed that the impact strength (a_n) was increased from 15 to 50, 100, and 115 KJ/m², respectively, when 5%, 10% and 20% SEBS-g-MAH were added to the PP/PET (90/10) blend. This super high impact strength might result from the special PP/PET

interfacial structure, in which the PET micro fibers were closely surrounded by the PP matrix, in a similar way as the effect described in¹⁸ for compatibilized blends of recycled PET and recycled HDPE. The unnotched impact strength (a_k) for the different compositions shows a similar behavior as a function of the compatibilizer content (results not shown here).

The use of a compatibilizer can alleviate the surface tension and the interface energy to improve the interfacial adhesion, which makes the dispersed PP particles finer and well-distributed in PET matrix. After the compatibility is improved, PP together with the compatibilizer act as a toughening materials for PET, which results in increasing the impact strength of the blend.¹⁷ The role of the SEBS part is to

improve the compatibility between the PET phase and the PP phase only by physical interaction, while the part of the anhydride groups of SEBS-g-MAH could react, to a certain extent, with the hydroxyl ends of PET chain, to give rise to a PET-co-SEBS-g-MAH copolymer.^{5,17}

Microhardness study

a) Pure PP/PET blends

Figure 8a illustrates the behavior of the microhardness H in pure PP/PET blends. For PET contents up to 20 %, the samples look uniform in aspect by visual inspection, and the hardness values are similar to that of pure PP. When the PET content is equal or higher than 80 %, samples look also uniform in aspect, hardness values becoming close to that of pure PET. Samples with PET content between 30 and 60 % clearly exhibit two different regions or phases, each one having the hardness value of each component. The sample with 70 % of PET presents a very high hardness

value (128 MPa). It was not possible to measure the hardness of the sample with 40 % PET because no clearly defined indentation appeared.

From Figure 8a, it is clear that, in case of pure blends, it has not been possible to obtain uniform materials under our processing conditions (see Experimental). However, none of the compatibilized blends showed this type of problem.

b) PP/PET blends + 5 % of SEBS-g-MAH

These blends behave in a different way from those without compatibilizer (see Figure 8b). Thus, for PET contents equal or higher than 70 %, the measured hardness values coincide with the calculated taking into account the composition, *i.e.*, these blends follow the additivity law. However, if the PET content is 50 % or less, the hardness values are even lower (about 44 MPa) than the value found for pure PP, *i.e.*, 54 MPa (see Figure 5a). Again, it was not possible to measure the hardness of the blend with 40 % of PET for the same reason as above indicated.

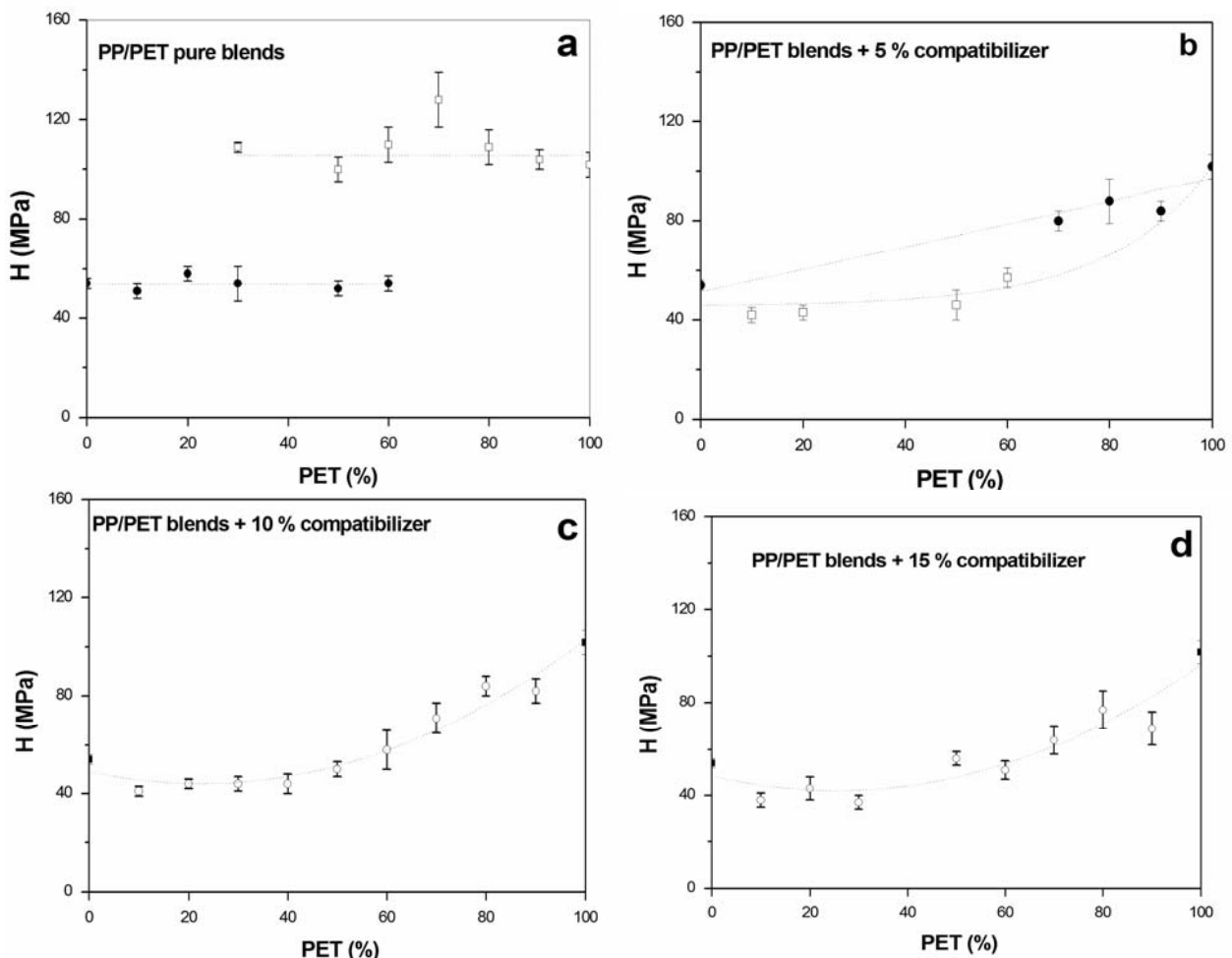


Fig. 8 – Microhardness H of: a) pure PP/PET blends; b) PP/PET blends + 5 % compatibilizer; c) PP/PET + 10 % compatibilizer; d) PP/PET blends + 15 % compatibilizer.

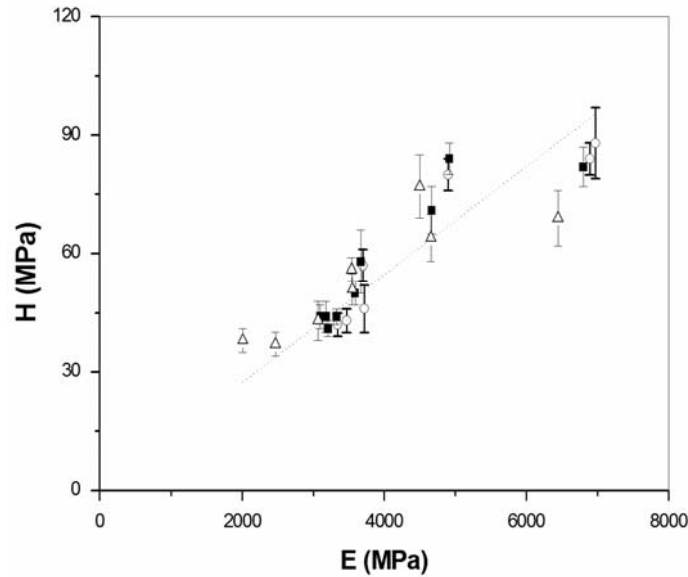


Fig. 9 – Relationship between Young's modulus E and microhardness H for the PP/PET compatibilized blends.

c) and d) PP/PET blends + 10 % or 15 % of SEBS-g-MAH

In all these blends, the hardness values increase with the increasing content of PET (see fig. 8c and 8d). But these values always keep lower than those predicted by the additivity law, this effect being more pronounced for higher SEBS-g-MAH content. The relationship between the Young's modulus E and the microhardness H of the compatibilized blends is illustrated in Fig. 9. From this plot, it can be derived the value $E/H = 73.2$. By comparing the influence of the PET and the compatibilizer content in the hardness H of the compatibilized blends, (see figs. 8b-8d), it is clear that these blends do not obey the additivity law of a binary blend as a function of composition:

$$H = H_1\Phi_1 + H_2(1 - \Phi_1) \quad (5)$$

where H_1 , H_2 , Φ_1 and $(1 - \Phi_1)$ are the hardness values of the blend components and their molar fractions, respectively. The results obtained for the compatibilized blends showed more or less constant H values for PET contents until 40-50 %, and for larger PET content, H increased again. In addition to this, the hardness of the blends decreased with increasing amounts of compatibilizer. These effects can be explained by the decrease in H_c^{PP} in the blends. In semicrystalline polymers, the relationship between H_c and l_c is given by:

$$H_c = H_c^\infty / (1 + b/l_c) \quad (6)$$

In this expression, H_c^∞ is the hardness of an infinitely thick crystal, and the b parameter is

defined as: $b = 2\sigma_e / \Delta h$. On the other hand, Δh is the energy needed to plastically deform the crystalline lamellar stacks.

As it was above told, the crystal thickness l_c is practically constant for both components in all the blends. Thus, the diminution in H_c value for the PP could be explained by an increase in the b parameter (eq. 6), through the surface free energy σ_e , which is related to the degree of order at the crystals surface.¹⁹ The value of σ_e could be increased by the blending process, or by the presence of the compatibilizer, constituted by amorphous chains of elastomeric character, or by a combination of both factors.¹⁰ These results are in agreement with the ones found by Hellati *et al.*²⁰

CONCLUSIONS

Blends of PET and PP result in materials with inferior mechanical properties because of the incompatibility between the two phases. By adding SEBS-g-MAH compatibilizer (a thermoplastic elastomer functionalized with maleic anhydride), the resulting materials show improved mechanical properties.

Some mechanical properties, as Young's modulus and stress at break, show higher values for the lower compatibilizer content used, *i.e.*, 5 % SEBS-g-MAH. However, the elongation at break and the impact strength are higher for the highest SEBS-g-MAH content, *i.e.*, 20 %wt. Improvements in the ductility of the blends have been observed due to the presence of the compatibilizer.

The decrease in the melt flow index MFI values for the compatibilized blends is due to the interaction between the compatibilizer and the polymers.

The thermal properties reveal that the crystallinity of PP and PET depends only on the composition. For the compatibilized blends, the percentage of crystallinity of both components slightly decreases with an increase of the compatibilizer content.

In case of compatibilized blends, the hardness behavior is explained by the assumption that Φ_e of the PP crystals notably increases due to the addition of SEBS-g-MAH, (amorphous material, constituted by short chains of elastomeric character), or to the blending process, or to a combination of both effects.

The results of the WAXS study carried out in the compression molded blends indicate that, under these conditions, only the PP component is able to crystallize, and its degree of crystallinity depends on the blend composition, being lower for higher PET and SEBS-g-MAH contents.

Acknowledgements: One of the authors (MEC) wishes to thank the Spanish Ministry of Science and Innovation MICINN for the financial support of this investigation (Grant MAT2009-07789).

REFERENCES

1. K. Jarukumjorn and S. Chareunkvun, *Suranaree. J. Sci. Technol.*, **2006**, *14*, 1-8.
2. B. Ballauri, M. Trabuio and F. P. La Mantia, "Recycling of PVC and mixed plastic waste", La Mantia FP (Ed.), Chem. Tec. Publishing, Toronto, Canada, 1996, p. 77-91.
3. R. Navarro, S. Ferrándiz, J. López and V.J. Seguí, *J. Mat. Process. Technol.*, **2008**, *195*, 110-116.
4. P. Potiyaraj, S. Tanpichai and P. Phanwiroj, *Adv. Mat. Res.*, **2012**, *488*, 109-113.
5. M. Heino, J. Kirjava, P. Hietaoja and J. Seppala, *J. Appl. Polym. Sci.*, **1997**, *65*, 241-249.
6. M. Y. Pedram, H. Veja, J. Retuert and R. Quijada, *Polym. Eng. Sci.*, **2003**, *43*, 960-964.
7. S.H. Jafari, A. Kalati-vahid, H. A. Khonakdar, A. Asadinezhad, U. Wagenknecht and D. Jehnichen, *EXPRESS. Polym. Lett.*, **2012**, *6*, 148-158.
8. R. Sarami, N.G. Ebrahimi and M.R. Kashani, *Iran. Polym. J.*, **2008**, *17*, 243-250.
9. R. Krache, D. Benachour and P. Potschke, *J. Appl. Polym. Sci.*, **2004**, *94*, 1976-1985.
10. R. Krache, D. Benachour, M. E. Cagiao, F. J. Baltá Calleja, R. K. Bayer and F. Tschöpe, *Int. J. Polym. Mater.*, **2003**, *52*, 939-956.
11. M. Ghafoori, N. Mohammadi and S. R. Ghaffarian, *Iran. Polym. J.*, **2006**, *15*, 747-755.
12. J. Maity, C. Jacob, S. Alam and R. P. Sing, *J. Comp. Mat.*, **2009**, *43*, 709-723.
13. F. J. Baltá Calleja and S. Fakirov, "Microhardness of Polymers, Solid State Science Series", Cambridge University Press (Ed), Cambridge, England, 2000, p 3. (look at reference no. 2)
14. ATHAS Databank: <http://athas.prz.rzeszow.pl> (accessed March 2013)
15. A. Flores, J. Aurrekoetxea, R. Gensler, H. H. Kausch and F. J. Baltá Calleja, *Colloid. Polym. Sci.*, **1998**, *276*, 786-793.
16. A. Celli and E. D. Zanotto, *Thermochim. Acta.*, **1995**, *269*, 191-199.
17. H. Zhang, W. Guo, Y. Yu, B. Li and Ch. Wu., *Eur. Polym. J.*, **2007**, *43*, 3662-3670.
18. Y. Lei, Q. Wu and Q. Zhang, *Compos. Part A- Appl S.*, **2009**, *40*, 904-912.
19. F. J. Baltá Calleja and S. Fakirov, "Microhardness of Polymers, Solid State Science Series", Cambridge University Press (Ed), Cambridge, England, 2000.
20. A. Hellati, D. Benachour, M. E. Cagiao, S. Boufassa and F. J. Baltá Calleja, *J. Appl. Polym. Sci.*, **2010**, *118*, 1278-1287.